P1.13

A STUDY OF VERTICAL LIQUID WATER PROFILES OF CLOUDS FROM IN-SITU MEASUREMENTS

Korolev A. V *, G. A. Isaac, J. W. Strapp, and S. G. Cober
Environment Canada, Toronto, ON, Canada

1. INTRODUCTION

Knowledge of the variability of cloud microphysical characteristics in the vertical is important for a variety of reasons. Profiles of liquid water content (LWC) affect the interaction of clouds with solar and infrared radiation and ultimately contribute to the radiation budget. Information about LWC profiles improves our understanding of the processes acting to form and maintain cloud systems. This understanding may lead to the improvement of numerical models and parameterization of clouds. The vertical distribution of liquid water and temperature inside supercooled clouds is important in the estimation of in-flight icing severity and aviation safety. At present in-situ airborne measurements provide the most accurate information about cloud microphysical characteristics. This information can be used for validation of numerical models and ground based and satellite remote sensing techniques.

The statistical characteristics of supercooled stratiform frontal clouds collected during five aircraft field campaigns are presented here. Effort was focused on an analysis of the statistics of cloud depths, liquid water path, and vertical distribution of liquid water and temperature inside clouds.

2. INSTRUMENTATION

Measurements of liquid water profiles were obtained using the National Research Council of Canada Convair-580 aircraft (Fig 1a), which was extensively equipped by the Environment Canada for cloud microphysical measurements. The following set of aircraft instruments was used to characterize the cloud environment: (1) a Nevzorov probe (Sky Tech Research, Inc.), was used for measurements of liquid (LWC) and total (ice + liquid) (TWC) water contents (Korolev et al. 1998); (2) a King probe for measurements of LWC (King et al. 1978); (3) a Rosemount Icing Detector (RICE) (BF Goodrich Aerospace Sensors Division) for detecting the presence of supercooled liquid water zones with LWC>0.01g/m^3 (Cober et al. 2001, Mazin et al. 2001); (4) PMS (Particle Measuring Systems, Inc.) OAP-2DC and OAP-2DP optical array probes for sizing and imaging cloud particles larger than approximately 100μm and identifying the presence of drizzle and rain drops using image recognition analysis; (5) two Rosemount total-air temperature probes (model 102DJ1CG) (Lawson and Cooper 1990, Friehe and Khelif,

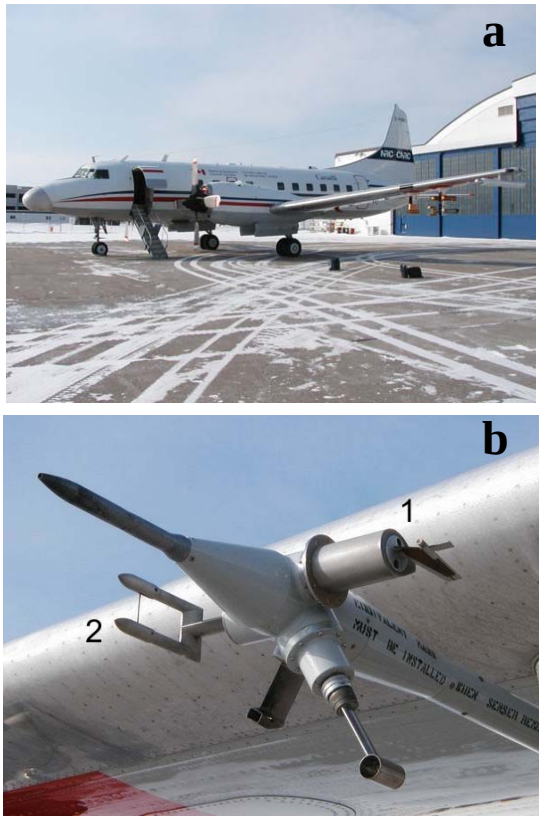

Figure 1. (a) The National Research Council of Canada Convair-580; (b) Convair-580 wing boom with the hot-wire instrumentation for cloud water measurements: Nevzorov LWC/TWC probe (1) and CSIRO King probe (2)

* *Corresponding author address*: Alexei Korolev, Environment Canada 4905 Dufferin Street, Toronto, Ontario, M3H5T4 Canada, alexei.korolev@ec.gc.ca

1992) and one reverse-flow air-temperature probe (Rodi and Spyers-Duran 1972); (6) a Rosemount 858 for measurements of wind gusts, altitude and airspeed; and (7) a Litton 9100 IRS for measurements of position and attitude, and contributing to wind calculations.

The goal of this analysis was to identify the time periods of aircraft climb and descent through cloud layers, and to then calculate the liquid water path (LWP) through each layer. In the context of this study, in mixed-phase clouds we considered only liquid fraction of the condensed cloud water in this calculation. Ice clouds and ice fraction of condensed water content in mixed clouds were disregarded. For the sake of simplicity, all clouds containing LWC will hereafter be referred to as "liquid", regardless if they contain ice particles or not.

The Nevzorov probe (Fig. 1b) was used as the primary instrument for the measurement of LWC. In order to avoid artifacts and misinterpretation of the data due to possible probe or data system malfunctions, the Nevzorov probe measurements always were compared with the RICE, King probe, PMS FSSP, OAP-2DC and OAP-2DP data. Calculations of the LWC from the Nevzorov probe data were made following the procedure described in Korolev et al. (2003). Several studies have shown that ice particles may cause a response on the LWC sensor (e.g. Korolev et al. 1998; Strapp et al. 1999; Cober et al. 2001, Korolev and Strapp 2002, Field et al. 2004). The residual effect of ice on the LWC sensor is due to the small amount of heat removed from the LWC sensor during impact with ice particles. The residual effect is characterised by the residual coefficient $\alpha = W_{liq}^{*} / W_{ice}$, where W_{liq}^{*} is the response of the LWC sensor to ice particles with a corresponding ice water content W_{ice}. In theory, the residual coefficient is usually estimated as $\alpha = W_{LWC}/W_{TWC}$, where W_{LWC} and W_{TWC} are the water contents measured in *ice* clouds with zero LWC by the LWC and TWC sensors, respectively. The value of the residual coefficient α depends on the size, shape and bulk density of ice particles, air speed, air and sensor temperatures, and it has been shown to vary from 0.01 to 0.5. Large α values are thought to be typical for a high concentration of small ice particles, and perhaps at high true airspeeds, as has been observed in measurements at the tops of thunderstorms (Strapp et al. 1999). In mid-latitude frontal clouds, the residual coefficient is usually close to α=0.18, which was the value used for this study.

3. DESCRIPTION OF THE DATA SET

The data were collected during five field campaigns: (1) the First Canadian Freezing Drizzle Experiment (CFDE 1) in March 1995, (2) the Third Canadian Freezing Drizzle Experiment (CFDE 3) in December 1997-February 1998 (Isaac et al., 2001), (3) the First Alliance Icing Research Study (AIRS1) December 1999-February 2000 (Isaac et al. 2001); (4) the Alliance Icing Research Study 1.5 (AIRS1.5) January 2003; (5) the Second Alliance Icing Research Study (AIRS2) November 2003-February 2004 (Isaac et al. 2005). During CFDE 1 the flights were conducted over Newfoundland and the East Coast of Canada, whereas CFDE 3 and AIRS (1, 1.5 and 2) were carried out over Southern Ontario and Quebec. All of the data summarized in this study were collected using the NRC Convair-580 aircraft.

The bulk of the data were sampled in stratiform clouds (*St, Sc, Ns, As, Ac*), associated with frontal systems. The airspeed of the airplane during sampling was approximately 100 ms^{-1}. The measurements were averaged over one-second time intervals, which corresponds to a spatial resolution of approximately 100 m. In total, 67 flights were included in the analysis. The duration of the flights was typically between 2 to 5 hours. The temperature of the liquid water profiles included in the analysis was limited to the range of 0^{o}C to -35^{o}C. The altitude of measurements ranged from 0 to 7 km. Profiles were accomplished both by using spiral and enroute climbs and descents. The aircraft vertical velocity during vertical soundings ranged from 2m/s to 18m/s and typically was approximately 5m/s.

The total number of separately analyzed stratiform layers was 584. Two cloud layers were considered distinct if the vertical distance between cloud top of the lower layer and the base of the upper layer exceeded 50 meters. Otherwise, the cloud was considered as a continuous single layer. In order to avoid misidentifying cloud fragments, typically observed near cloud boundaries, cloud layers with a depth ΔZ<50m were excluded from our analysis. The sensitivity threshold for the detection of liquid clouds was set to 0.005g/m^3. Clouds with LWC<0.005g/m^3 were disregarded, and considered as a clear air.

Since the flight campaigns discussed here were carried out during the cold seasons, most of the clouds sampled were supercooled. Therefore, for example, the statistics of the LWC profiles should not be used for validation of numerical models or remote sensing related to warm frontal clouds.

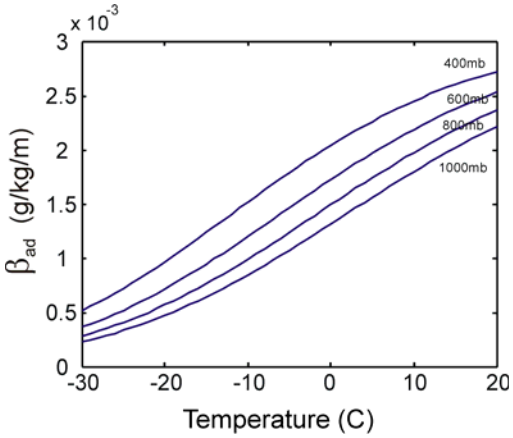

Figure 2. Dependence of the vertical gradient of adiabatic LWC on temperature, for various pressures.

4. RESULTS

4.1 *Distribution of LWC within cloud layers*

Theoretical calculations suggest that LWC increases with altitude for the case of clouds formed by adiabatic lifting, and its value a unique function of the height above the cloud base. The vertical gradient of LWC $\beta_{ad} = \left(\frac{dW}{dZ}\right)_{ad}$ is a relatively weak function of temperature and pressure (Fig. 2), and for dZ of a few hundred meters, β_{ad} stays approximately constant. Therefore, the LWC is expected to change linearly with altitude in relatively thin clouds (ΔZ<500m).

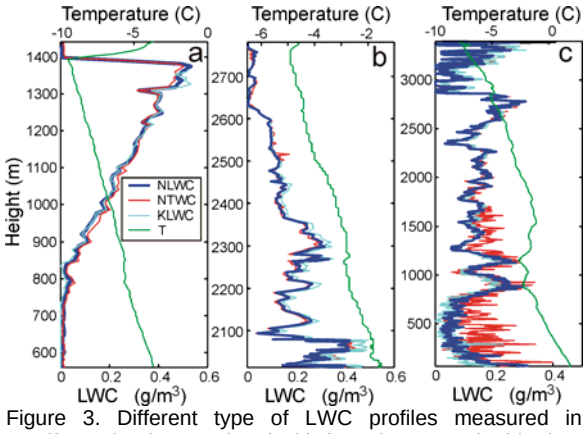

Figure 3. Different type of LWC profiles measured in stratiform clouds associated with frontal systems in this data set (a) St-Sc 15 December 1995; Southern Ontario; (b) Ns, 22 March 1995; Newfoundland; (c) Ns, 11 November 2003; Southern Ontario.

In real clouds the LWC profile is disturbed by the entrainment of dryer air, mixing, precipitation fallout, and radiation effects. For the current data set, it was found that LWC can both increase (Fig. 3a) and decrease (Fig. 3b) towards the cloud top. In many cases the LWC profiles may have several distinct maxima (Fig. 3c).

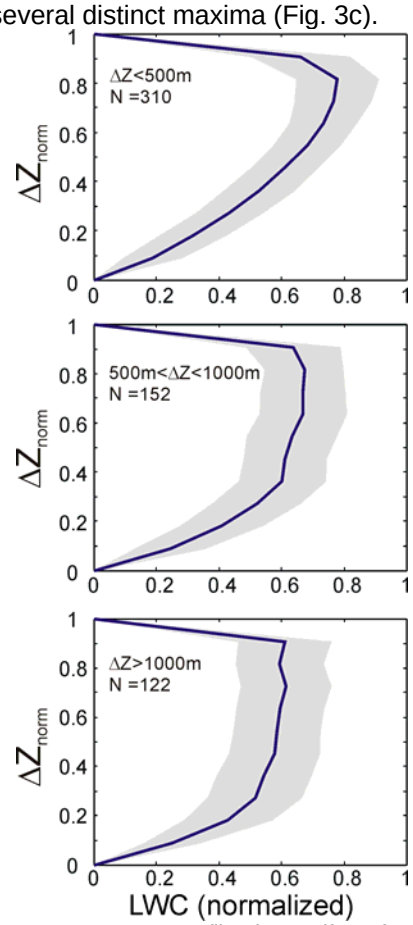

Figure 4. Average LWC profiles in stratiform frontal cloud layers for (a) ΔZ <500m (b) 500m< ΔZ <1000m and (c) ΔZ>1000m. LWC was normalized to the maximum value in each profile, distance above base was normalized to the depth of the cloud layer. The grey shaded area shows standard deviation of LWC data.

The average LWC profiles calculated for the layers with ΔZ<500m, 500<ΔZ<1000m and ΔZ>1000m are shown in Fig. 4. Since the cloud depth and LWC varies over a wide range, the elevation above cloud base was normalized to the cloud depth (ΔZ), and LWC was normalized to the maximum LWC (W_{max}). As seen from Fig. 4a, in relatively thin cloud layers with ΔZ<500m, the LWC changes nearly linearly in the lower and middle part of the layer, and the LWC has a distinct maximum near the cloud top at dZ~0.8. The averaged LWC profile for cloud layers with the depths over 500m (Fig.4b,c) have approximately constant LWC at 0.4<ΔZ_{norm}<0.9.

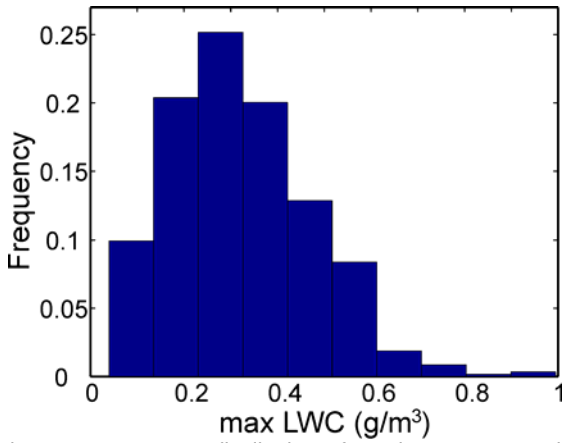

Figure 5. Frequency distribution of maximum 100m-scale LWC in frontal cloud layers at 0.1 g/m^3 intervals.

The frequency distribution of maximum LWC (at a ~100 m horizontal averaging scale) in the supercooled cloud layers is shown in Fig. 5, with the overall maximum LWC being W_{max}=1.0 g/m^3. The mean and median W_{max} are equal to 0.32 g/m^3 and 0.31 g/m^3, respectively.

The average LWC in cloud layers was found not to depend on the cloud depth for clouds with ΔZ>500m, and it is approximately equal to 0.14 gm^{-3} (Fig. 6).

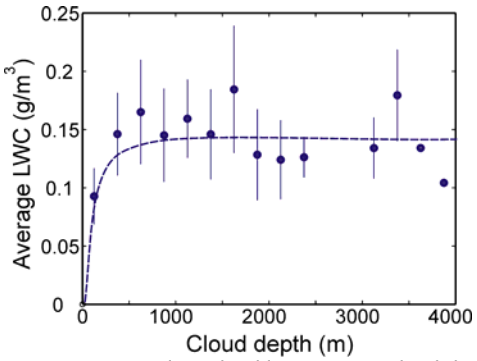

Figure 6. Average LWC in a cloud layer versus cloud depth. Vertical bars indicate standard deviations of measurements.

4.2 *Thickness of supercooled cloud layers*

The depth of continuous supercooled cloud layers varies from a few dozen meters to a few kilometers. One example of a deep cloud layer with a ΔZ ~3500m is shown in Fig. 3c. Usually deep continuous liquid cloud layers have several distinct LWC maxima.

Fig. 7 shows the frequency distribution of supercooled liquid layer depths in frontal clouds. As seen from Fig. 7 more than 50% of cloud layers have depths less than 500m. The maximum thickness of a continuous liquid layer was found to be 4500m.

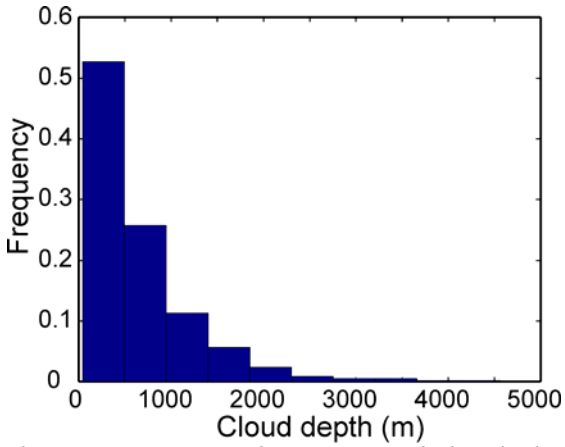

Figure 7. Frequency of occurrence of the depth of supercooled stratiform frontal cloud layers in 500m bins.

Fig. 8 shows the distribution of cloud depths for different temperature intervals. Fig. 8 indicates that the thickness of clouds has a tendency to decrease with decreasing temperature. Fig. 9 shows the dependence of the cloud depth on average temperature of the layer, illustrating that the thickness of stratiform cloud decreases with decreasing temperature. Thus, below -25^{o}C. stratiform clouds were found to form thin layers having a depth usually no more than 100 m.

The overall average and median depth of supercooled cloud layers were 660m and 470m, respectively.

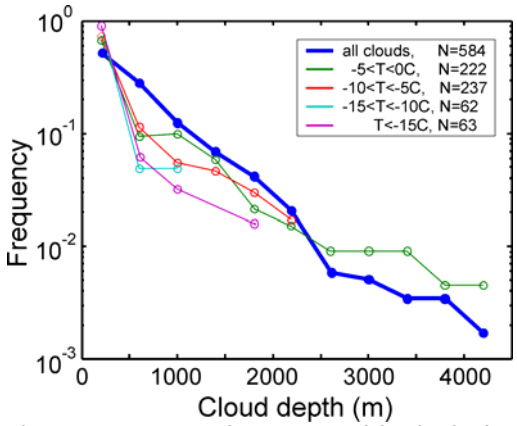

Figure 8. Frequency of occurrence of the depth of stratiform layers in 400 m bins, for different temperature intervals. Thick blue line indicates the same distribution as in Fig.7

4.3 *Temperature distribution in supercooled cloud layers*

The air temperature in most supercooled liquid layers decreases towards cloud top. However some cloud layers may have an

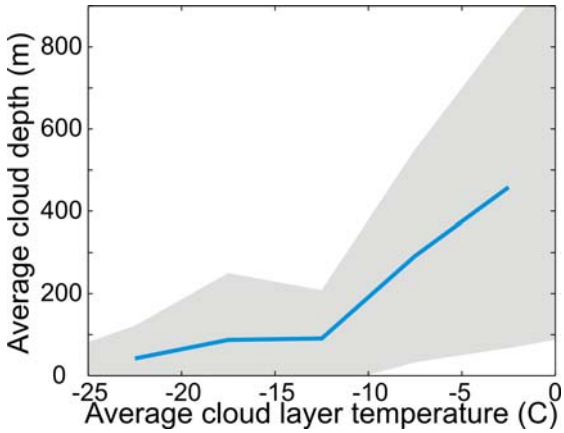

Figure 9 Average continuous cloud thickness of supercooled liquid layers, versus average temperature of the layer.

embedded temperature inversion, where the temperature increases with height. This proves to be generally true in most frontal clouds. The fractions of the cloud layers where the temperature of the cloud top (T_{top}) is colder, equal, or warmer than at cloud base (T_{base}) are 0.66, 0.17, and 0.17, respectively. The temperatures T_{top} and T_{base} were classified as "equal" if $|T_{top}-T_{base}|<0.5^{o}$C. The temperature at the top of deep cloud layers (ΔZ>2km) is usually no colder than -10^{o}C.

4.4 *Liquid water path*

Fig. 10 shows the cumulative probability of LWP derived from the in-situ measurements of the vertical distribution of LWC in cloud layers. The results in Fig. 10 are expressed terms of absolute probabilities of LWP larger than a given value for a vertical traverse through the cloud layer. The in-situ measurements of LWP (blue circles) are compared with LWP derived from ground-based 37 GHz microwave radiometer measurements (red circles) adapted from Koladev et al. (1999). The radiometer provides a continuous estimate of liquid water path (LWP), the integrated amount of liquid in a column above the radiometer. Koldaev et al. (1999) collected their measurements over one winter season near Toronto, Canada. The slopes of the two distributions are quite similar. The offset between the two lines is likely due to the fact that the radiometer data are absolute probabilities that include periods of no cloud, whereas the airborne data are conditional probabilities where cloud must be present. Overall, the good agreement between the slopes of the lines is an encouraging validating result for the use 37 GHz radiometers for LWP measurements.

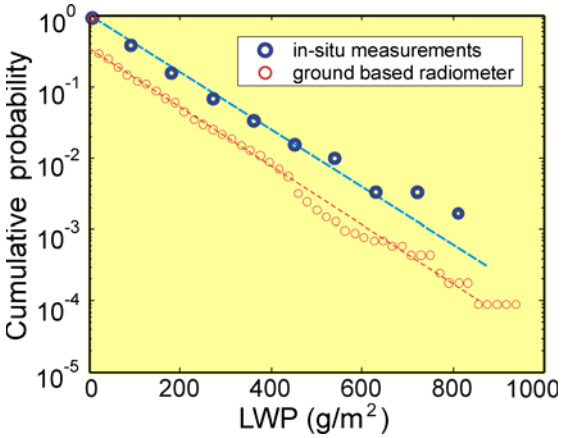

Figure 10. Frequency of occurrence of the liquid water path (LWP) of stratiform frontal cloud layers(blue circles), and absolute probability of LWP based on previous ground-based measurements with a 37GHz radiometer (Koldaev et al. 1999) (red circles).

Fig. 11 shows the dependence of the LWP on the depth of the cloud layer. As seen in this figure, LWP is a nearly linear function of the cloud thickness, and it can be describe as

$$LWP=0.14\Delta Z, \qquad (1)$$

where ΔZ is the thickness of a cloud layer in meters, and LWP is in g/m^{2}. This is of course completely consistent with the observation above of an average LWC of cloud layers of ΔZ>500m, independent of depth, of 0.14 gm^{-3}.

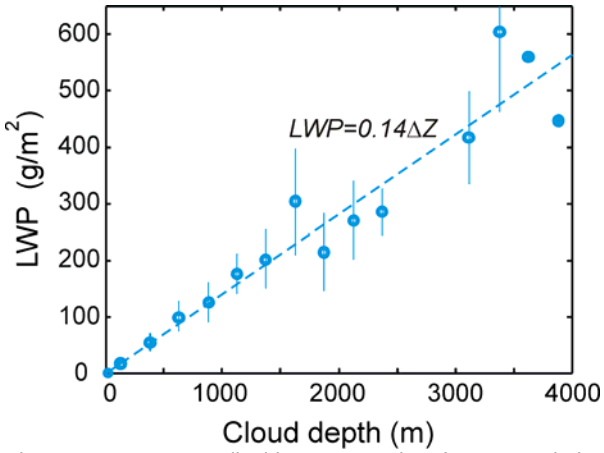

Figure 11. Average liquid water path of supercooled stratiform frontal cloud layers, as a function of cloud depth.

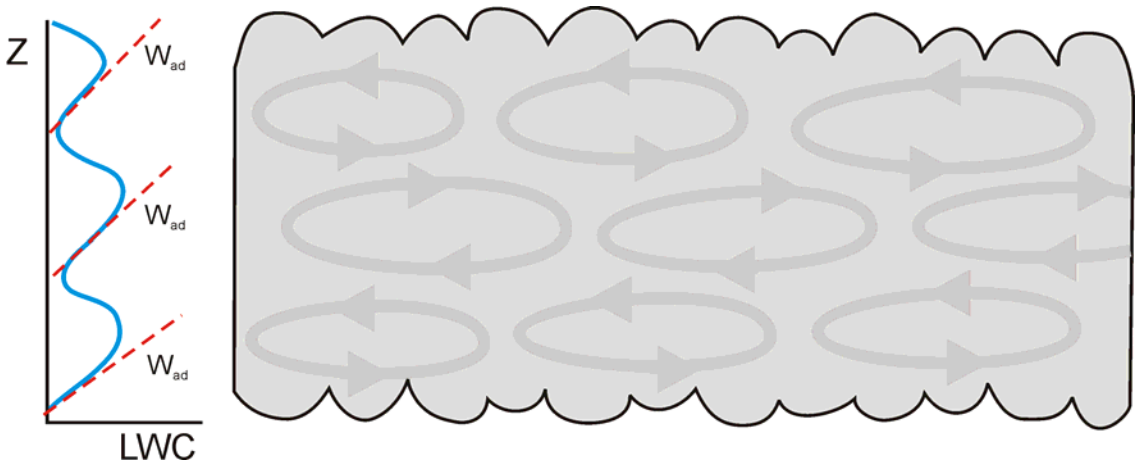

Figure 12. Conceptual diagram of the formation multi-maxima LWC profiles in deep frontal clouds.

5 DISCUSSION

This study of cold winter frontal clouds has shown that the depths of continuous stratiform layers may reach 3-4 km (Figs. 7-8). The liquid water profile in such clouds is essentially non-adiabatic, and LWC near the cloud tops of deepcloud layers (ΔZ>2km) is usually 5 to 10 times lower than the adiabatic LWC. Typically the LWC profile in deep cloud layers has several distinct LWC maxima (Fig. 3c). Such a vertical structure of LWC suggests that the vertical transport of cloud parcels in deep frontal clouds is limited. In other words cloud parcels may not travel from cloud base to cloud top, like in shallow stratocumulus layers, but rather oscillate around certain levels. Such oscillations may be arranged in a form of closed cells and be generated by gravity waves or wind shear typical for frontal systems. A conceptual diagram of dynamical structure explaining multi-maximum LWC profiles in deep frontal LWC layers is shown in Fig.12. Each of these cells may generate a quasi-adiabatic profile of LWC. The characteristic vertical extent of such cells (ΔH_c) can be estimated from the maximum LWC, which will be reached in the upper part of the cells, as follows:

$$\Delta H_c = W_{max}/\beta_{ad} \qquad (2)$$

As found in section 4.1, the average value of W_{max} =0.3g/m^3. Assuming β_{ad} =1.2 10^{-4}gm-^{3}m^{-1} at T=-5C and P=700mb, Eq.2 yields ΔH_c~250m. Taking into account the non-adiabatic nature of LWC due to mixing, precipitation fallout, etc., the actual size of the cells will probably be deeper than that calculated above, consistent with the depth of quasi-adiabatic single layers ΔZ~500m.

6 CONCLUSIONS

Based on the analysis of 584 supercooled cloud layers the following conclusions have been obtained:

1. Shallow stratiform clouds (ΔZ<500m) in frontal systems tend to have a quasi-linear LWC profile, whereas deep layers (ΔZ>500m) have a constant LWC in their central and upper regions.
2. The average LWC in deep cloud layers does not depend on ΔZ and is approximately equal 0.14g/m^3.
3. The depth of cloud layers decreases with decreasing average layer temperature. Typically for clouds with an average temperature T=-25C, the cloud depth does not exceed 100m.
4. A good agreement between the statistical distributions of LWP derived from in-situ LWC profiles and those measured in previous experiments from ground based 37GHz radiometers was obtained.
5. Deep frontal liquid layers usually have LWC profiles with multiple local maxima in the vertical. Such profiles may be explained by a multi-cellular circulation, with a characteristic vertical dimension of such cells of the order of a few hundred meters.

Acknowledgments

The authors would like to acknowledge their colleagues at the National Research Council of Canada because all the measurements reported in this paper were made using the NRC Convair-580. Funding was also provided by many different agencies such as the National Initiative

Fund of the Search and Rescue Secretariat, Transport Canada, FAA, NASA and the Boeing Commercial Airplane Group.

References

Friehe, C.A., and D. Khelif, 1992: Fast-Response Aircraft Temperature Sensors. *J. Atmos. Oceanic Techn.,* **9**, 784–795

Isaac, G.A., S.G. Cober, J.W. Strapp, D. Hudak, T.P. Ratvasky, D.L. Marcotte, and F. Fabry 2001a: Preliminary results from the Alliance Icing Research Study (AIRS). *AIAA 39th Aerospace Sci. Meeting and Exhibit*, Reno Nevada, 8-11 January 2001, AIAA 2001-0393.

Isaac, G.A., S.G. Cober, J.W. Strapp, A.V. Korolev, A. Tremblay, and D.L. Marcotte, 2001b: Recent Canadian research on aircraft in-flight icing. *Canadian Aeronautics and Space Journal*, **47**, 213-221.

Isaac, G.A., J.K. Ayers, M. Bailey, L. Bissonnette, B.C. Bernstein, S.G. Cober, N. Driedger, W.F.J. Evans, F. Fabry, A. Glazer, I. Gultepe, J. Hallett, D. Hudak, A.V. Korolev, D. Marcotte, P. Minnis, J. Murray, L. Nguyen, T.P. Ratvasky, A. Reehorst, J. Reid, P. Rodriguez, T. Schneider, B.E. Sheppard, J.W. Strapp, and M. Wolde, 2005: First results from the Alliance Icing Research Study II. *AIAA 43rd Aerospace Sci. Meeting and Exhibit*, Reno Nevada, 11-13 January 2005, AIAA 2005-0252.

Isaac, G.A., M. Bailey, S.G. Cober, N. Donaldson, N. Driedger, A. Glazer, I. Gultepe, D. Hudak, A. Korolev, J. Reid, P. Rodriguez, J. W. Strapp and F. Fabry, 2006: Airport Vicinity Icing and Snow Advisor. *AIAA 44rd Aerospace Sci. Meeting and Exhibit*, Reno Nevada, 9-12 January 2006, AIAA-2006-1219.

Cober, S.G., Isaac, G.A., and A.V. Korolev, 2001: Assessing the Rosemount Icing Detector with in-situ measurements. *J. Atmos. Oceanic Technol.,* **18**, 515-528

Cober, S.G., Isaac, G.A. Korolev, A.V. And Strapp, J.W., Assessing Cloud Phase Conditions, *J. Appl. Meteor*., Vol. 40, 2001, pp. 1967-1983

King, W. D., D. A. Parkin and R. J. Handsworth, 1978: A hot-wire water device having fully calculable response characteristics. *J. Appl. Meteor.*, **17,** 1809-1813.

Knollenberg, R. G. 1981 Techniques for probing cloud microstructure. In: *Clouds, their formation, Optical properties, and Effects*, P. V Hobbs, A. Deepak, Eds. Academic Press, 495 pp

Koldaev, A., T.B. Low, and J.W. Strapp. Microwave Measurements of Cloud Liquid Water Path and Average In-cloud Temperature at King City, Ontario, Winter 96/97. Transport Canada Report TP14104, March 1999, 94 pp.

Korolev, A.V., J.W. Strapp, G.A. Isaac, and A. Nevzorov, 1998: The Nevzorov airborne hot wire LWC/TWC probe: Principles of operation and performance characteristics. *J. Atmos. and Ocean. Technol*., 15, 1495-1510.

Korolev, A.V., G.A. Isaac, S. Cober, J.W. Strapp, and J. Hallett, 2003: Microphysical characterization of mixed-phase clouds. *Quart.J.Roy.Meteor.Soc.,* **129**, 39-66

Korolev, A.V., J. W. Strapp, 2002: Accuracy of Measurements of Cloud Ice Water Content by the Nevzorov Probe. *AIAA 40th Aerospace Sci. Meeting and Exhibi*t, Reno, Nevada, 14-17, January 2002, AIAA 2002-0679

Lawson R.P., and W.A. Cooper, 1990: Performance of Some Airborne Thermometers in Clouds. *J. Atmos. Oceanic Technol.,* **7**, 480–494.

Mazin, I. P., A. V. Korolev, A. Heymsfield, G. A. Isaac, and S. G. Cober, 2001: Thermodynamics of icing cylinder for measurements of liquid water content in supercooled clouds. *J. Atmos. Oceanic Technol.,* **18**, 543-558.

Rodi, A.R., and P.A. Spyers-Duran. 1972: Analysis of Time Response of Airborne Temperature Sensors. *J. Appl. Meteor.* **11**, 554–556.

Strapp, J. W., P. Chow, M. Maltby, A. D. Bezer, A. Korolev, I. Stromberg and J. Hallett, 1999: Cloud Microphysical Measurements in Thunderstorm Outflow Regions During Allied/ BAE 1997 Flight Trials. *AIAA 37th AIAA Aerospace Sciences Meeting and Exhibit*, Jan 11-14, 1999, Reno, NV. AIAA 99-0498